Body fluid analog chlorination: Application to the determination of disinfection byproduct formation kinetics in swimming pool water

Lucie Tsamba, Nicolas Cimetiere, Dominique Wolbert, Olivier Correc, Pierre Le Cloirec

Body fluid analog chlorination: Application to the determination of disinfection byproduct formation kinetics in swimming pool water

Lucie Tsamba[1,2,*], Nicolas Cimetière[1], Dominique Wolbert[1], Olivier Correc[2], Pierre Le Cloirec[1]

1. Rennes University, ENSCR, CNRS, ISCR – UMR 6226, F – 35000 Rennes, France

2. Scientific and Technical Center for Buildings, 11 rue Henri Picherit, BP 82341, 44323 Nantes Cedex 3, France

---

* Corresponding author. E-mail: lucie.tsamba@cstb.fr (Lucie Tsamba)

Abstract

Disinfection by-products (DBPs) are formed in swimming pools by the reactions of bather inputs with the disinfectant. Although a wide range of molecules has been identified within DBPs, only few kinetic rates have been reported. This study investigates the kinetics of chlorine consumption, chloroform formation and dichloroacetonitrile formation caused by human releases. Since the flux and main components of human inputs have been determined and formalized through Body Fluid Analogs (BFAs), it is possible to model the DBPs formation kinetics by studying a limited number of precursor molecules. For each parameter the individual contributions of BFA components have been quantified and kinetic rates have been determined, based on reaction mechanisms proposed in the literature. With a molar consumption of 4 mol Cl_2/mol, urea is confirmed as the major chlorine consumer in the BFA because of its high concentration in human releases. The higher reactivity of ammonia is however highlighted. Citric acid is responsible for most of the chloroform produced during BFA chlorination. Chloroform formation is relatively slow with a limiting rate constant determined at 5.50×10^{-3} L/mol/sec. L-histidine is the only precursor for dichloroacetonitrile in the BFA. This DBP is rapidly formed and its degradation by hydrolysis and by reaction with hypochlorite shortens its lifetime in the basin. Reaction rates of dichloroacetonitrile formation by L-histidine chlorination have been established based on the latest chlorination mechanisms proposed.

Moreover, this study shows that the reactivity toward chlorine differs whether L-histidine is isolated or mixed with BFA components.

Keywords: Disinfection by-products

Kinetic modeling

Body fluid analog

Swimming pools

Introduction

Because of its residual disinfection capacity, chlorine is used in most swimming pool water treatment processes to ensure a good microbiological water quality. However, the formation of irritating or potentially toxic chlorinated disinfection by-products (Cl-DBPs) by reaction of chlorine with organic matter has been highlighted by many studies in the last 40 years (Beech, 1980; Florentin et al., 2011; Zwiener et al., 2007). Bathers and lifeguards are exposed to Cl-DBPs mainly through inhalation of volatile compounds or through dermal absorption (Erdinger et al., 2004; Lévesque et al., 1994). The exposure assessment and prediction require a model for the formation and degradation kinetics of Cl-DBPs in swimming pool water.

One of the major difficulties lies in the complex composition of the pollution released by bathers in the pool. Both the nature and amount of these organic compounds depend on various parameters, such as water temperature or bathers hygiene (Bessonneau et al., 2011; Keuten et al., 2012). Few studies described the amount of Cl-DBPs generated by the particles or by the pharmaceutical and personal care products released by bathers in the pools (Kim et al., 2002; Manasfi et al., 2017a; Teo et al., 2015). Most studies addressing DBP precursors in swimming pool focused on the dissolved human pollution, which consists mainly of urine and sweat, so that its responsibility for the production of large amounts of Cl-DBPs has now been well established (Bessonneau et al., 2011; Hureiki et al., 1994; Kim and Han, 2011).

Moreover, many studies have focused on urine and sweat compositions and on the quantities released in swimming pools (Putnam, 1971; WHO, 2006), leading to the formulation of Body Fluid Analogs (BFAs).

BFA solutions consist of the main components of human body fluids and they are mainly used to simulate the anthropogenic pollution in pilot-scale or bench-scale experiments. The most widely used composition has been suggested by Judd and Bullock (2003). This solution has the advantage to yield representative amounts of Cl-DBPs while involving only 7 components, namely urea, ammonia, creatinine, L-histidine, citric acid, uric acid and hippuric acid.

As the number of precursor molecules is limited to 7, a mechanistic approach can be considered, since it produces more reliable models. However, the chlorination kinetics and DBPs formation potentials of the BFA components have been unequally studied. Ammonia chlorination kinetics has been determined within the scope of the breakpoint chemistry (Jafvert and Valentine, 1992). Urea, which is known to be a urine component responsible for the formation of large amounts of trichloramine, has been widely studied since 1980, considering the health concerns raised by this DBP. Creatinine and L-histidine have been less studied but chlorination mechanisms have been proposed in the literature. The formation of chloroform and dichloroacetonitrile by L-histidine chlorination as well as the methylamine formation by creatinine chlorination have been explained (Li et al., 2017; Liu et al., 2017; Tachikawa et al., 2005). Finally, only few have focused on citric, uric and hippuric acids. Citric acid has been reported to produce large amounts of chloroform, whereas uric acid chlorination seems to be responsible for the production of high cyanogen chloride quantities (Larson and Rockwell, 1979; Lian et al., 2014). The formation potentials of the BFA components have been addressed for specific DBPs by few studies. Kanan and Karanfil (2011) described the important molar yields of citric acid for chloroform, dichloroacetic acid and trichloroacetic acid. However, individual contributions taking concentrations of the BFA formulation into account have not been determined, and kinetical aspects have not been considered by Kanan and Karanfil.

This article focuses on the formation of the main volatile DBPs in swimming pools (trihalomethanes and haloacetonitriles). Since bromination mechanisms of the BFA components remain largely unknown, this study focuses only on the formation of chlorinated-DBPs (chloroform and dichloroacetonitrile). Even if the brominated DBPs are more toxic and may be observed in fresh water or seawater pools (Manasfi et al., 2017b), their concentrations in most swimming pools are drastically lower than the Cl-DBPs concentrations.

Chloroform (TCM) and dichloroacetonitrile (DCAN) have been chosen as target molecules because of their different stabilities. Chloroform (TCM) is an ultimate, volatile and very stable Cl-DBP, which formation kinetics has been reported to be slow (Arnold et al., 2008; Blatchley et al., 2003). On the contrary, dichloroacetonitrile (DCAN) has been proven to degrade quickly through hydrolysis and through reaction with hypochlorite (Yu and Reckhow, 2017, 2015). This study identified the main precursors of TCM and DCAN within the BFA. The DBPs formation modeling was based on the specific chlorination study of the main precursors. Literature data such as chlorination mechanisms were coupled with experimental data from this study in order to determine kinetic rate constants. The resulting models were validated by comparison with the data provided by BFA chlorination experiments. Modeling the DBPs formation kinetics is the first step allowing to predict DBPs occurrence in pool water and air. Then the hydrodynamic parameters have to be taken into account to accurately predict concentration variations in water and air (Judd and Black, 2000; Peng et al., 2016; Schmalz et al., 2011). This method already predicted trichloramine occurrence in swimming pool water and air (Gérardin et al., 2015).

1. Materials and methods

Ultra pure water (UPW) produced by a ElgaPureLab System (resistivity 18.2 MΩ.cm, TOC< 50 µg C/L) was used for the preparation of all solutions and dilutions.

1.1 BFA chlorination

The BFA solution (**Table 1**) was freshly prepared according to Judd and Bullock composition the day before starting chlorination experiments. To overcome solubility difficulties, uric and hippuric acids were solubilized in approximately 20 mL of ultrapure water supplemented with 1 mL of a sodium hydroxide solution (5 mol/L). The pH of the final solution was adjusted to 7 with HCl.Sodium hypochlorite stock solutions (≈ 1 mol/L, Fisher Scientific) were regularly titrated iodometrically.

Chlorinated solutions were prepared in a 1 L volumetric flask by diluting the BFA mix or individual stock solutions in 50 mL of a 0.2 mol/L phosphate buffer (pH = 7.5 ± 0.1). Chlorine was added and the volume was adjusted to 1 L with ultrapure water. In the case of the BFA mix, the total organic carbon (TOC) concentration of the chlorinated solution reached 4 mg/L. The concentration of each BFA component in the final solution is indicated in **Table 1**. After chlorine addition, the solution was divided into a series of 60 mL amber glass bottles filled without headspace and placed in a 27°C ± 2°C thermostated bath. For contact times longer than 1000 hr, bottles were placed in a thermostated chamber at 27°C ± 1°C. All chlorination experiments are summarized in Appendix A.

Table 1 Body Fluid Analog (BFA) composition

Compound	CAS	Developed formula	Initial concentration in the chlorinated solution (individual and mix) (mmol/L)	TOC (mg/L)	% of total TOC	TN (mg/L)	% of total TN
Ammonium chloride	7664-41-7	NH_4Cl	2.88×10^{-2}	0	0	0.40	5.9
Urea	57-13-6	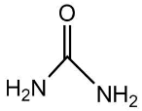	1.90×10^{-1}	2.28	56.7	5.3	79
L-Histidine	71-00-1	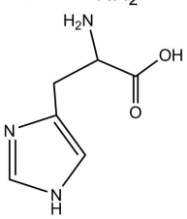	6.01×10^{-3}	0.036	0.9	0.25	3.7
Creatinine	60-27-5	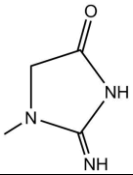	1.23×10^{-2}	0.594	14.8	0.52	7.7

Citric acid	77-92-9	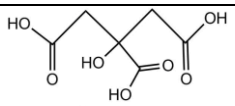	2.57×10^{-3}	0.185	4.6	0	0
Uric acid	69-93-2	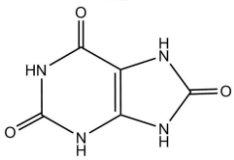	2.24×10^{-3}	0.134	3.33	0.13	1.9
Hippuric acid	495-69-2	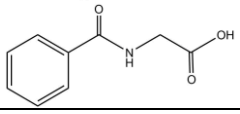	7.35×10^{-3}	0.793	19.7	0.10	1.5

Since the kinetics and mechanism of ammonia chlorination was extensively reviewed (Jafvert and Valentine, 1992; Qiang and Adams, 2004; Weil and Morris, n.d.), no chlorination experiment was carried on ammonia. The model published by Jafvert and Valentine (Jafvert and Valentine, 1992) was directly implemented in the BFA chlorination model.

1.2 Analytical methods

For each sampling point a 60-mL bottle was opened and 10 mL were immediately transferred into a 20 mL-headspace vial, quenched with 60 µL of a sodium thiosulfate solution (0.2 mol/L) and acidified with 60 µL of phosphoric acid (85%, Merck).

Free chlorine was measured by the DPD colorimetric method using a Shimadzu UV-1280 spectrophotometer (APHA, 2005). The quantification limit was 0.1 mg/L as Cl_2. If necessary, solutions were diluted with ultrapure water before analysis to reach a free chlorine concentration lower than 5 mg/L as Cl_2.

TCM and DCAN were measured by headspace GC-MS (Clarus 500, Perkin-Helmer). Vials were heated in the headspace oven (Perkin-Elmer) at 60°C for 10 min before injection. Separation was achieved with a FFAP capillary column (25 m × 0.15 mm i.d. × 0.25 µm) pressurized at 35 psi. Temperature for the GC oven started at 40°C for 5 min then rose to 120°C at 10°C/min and held for 5 min. The source temperature was set to 250°C. Standard solutions (2000 µg/mL, Sigma-Aldrich) were used to prepare external standards. TCM and DCAN were identified using full-scan analysis and they were quantified in Single Ion Monitoring (SIM) mode using ions at *m/z* = 83 and 74 respectively. Quantification limits were 5 µg/L and 2 µg/L

for TCM and DCAN respectively. Relative standard deviations (RSD) were below 5% (n=3) for both analyses.

1.3. Kinetic modeling

Kinetic modeling was performed on COPASI software v4.16. Kinetic rates were fitted either with chlorination experiment results from this study or with experimental data from the literature, using evolutionary programming. Acid base equilibria were supposed to be instantaneously reached. All equilibrium constants and literature sources are indicated in **Table 2**. The model includes 55 reactions, 7 precursors and a total of 64 molecules.

Table 2 Reaction rates of the model.

Reaction	Rate or equilibrium constant	Source*	Reaction label
$H_2O = H^+ + OH^-$	K_e=10^{-14} mol/L		(1)
$Cl_2 = HOCl + H^+ + Cl^-$	K= 3.94×10^{-4} mol^2/L^2 (25°C)	(Connick and Chia, 1959)	(2)
$HOCl = ClO^- + H^+$	K= 2.90×10^{-8} mol/L (25°C)	(Morris, 1966)	(3)
$NH_4^+ = NH_3 + H^+$	K=5.75×10^{-10} mol/L (25°C)	Bates and Pinching, 1950	(4)
$C_6H_8O_7 = C_6H_7O_7 + H^+$	K= 7.40×10^{-4} mol/L	(Bates and Pinching, 1949)	(5)
$C_6H_7O_7 = C_6H_6O_7 + H^+$	K= 1.73×10^{-5} mol/L	(Bates and Pinching, 1949)	(6)
$C_6H_6O_7 = C_6H_5O_7 + H^+$	K= 3.98×10^{-7} mol/L	(Bates and Pinching, 1949)	(7)
HOCl -> Cl^- + X	k= 4.42×10^{-7} sec^{-1}	BFA90	(8)
HOCl + NH_3 -> NH_2Cl + H_2O	k=4.17×10^6 L/mol/sec(25°C)	(Jafvert and Valentine, 1992)	(A1)
HOCl + NH_2Cl -> $NHCl_2$ + H_2O	k= 2.77×10^2 L/mol/sec (25°C)	(Jafvert and Valentine, 1992)	(A2)
HOCl + $NHCl_2$ -> NCl_3 + H_2O	k= 1.70×10^3 L/mol/sec (25°C)	(Jafvert and Valentine, 1992)	(A3)
NH_2Cl + H_2O -> HOCl + NH_3	k= 2.11×10^{-5} sec^{-1}(25°C)	(Jafvert and Valentine, 1992)	(A4)
$NHCl_2$ + H_2O -> NH_2Cl + HOCl	k=7.60×10^{-7} sec^{-1}(25°C)	(Jafvert and Valentine, 1992)	(A5)
2 NH_2Cl -> $NHCl_2$ + NH_3	k= 5.22×10^{-3} L/mol/sec (25°C)	(Jafvert and Valentine, 1992)	(A6)
$NHCl_2$ + NH_3 + H^+ -> 2 NH_2Cl + H^+	k= 6.00×10^3 L^2/mol^2/sec (25°C)	(Jafvert and Valentine, 1992)	(A7)
$NHCl_2$ + OH^- -> I	k= 1.11×10^2 L/mol/sec (25°C)	(Jafvert and Valentine, 1992)	(A8)
I + $NHCl_2$ -> HOCl + P	k= 2.78×10^4 L/mol/sec (25°C)	(Jafvert and Valentine, 1992)	(A9)

$I + NH_2Cl \rightarrow P$	$k = 8.33\times10^{3}$ L/mol/sec (25°C)	(Jafvert and Valentine, 1992)	(A10)
$NH_2Cl + NHCl_2 \rightarrow P$	$k = 1.52\times10^{-2}$ L/mol/sec (25°C)	(Jafvert and Valentine, 1992)	(A11)
$NHCl_2 + NCl_3 + OH^- \rightarrow 2\ HOCl + P$	$k = 5.56\times10^{10}$ $L^2/mol^2/sec$ (25°C)	(Jafvert and Valentine, 1992)	(A12)
$NH_2Cl + NCl_3 + OH^- \rightarrow HOCl + P$	$k = 1.39\times10^{9}$ $L^2/mol^2/sec$ (25°C)	(Jafvert and Valentine, 1992)	(A13)
$NHCl_2 + ClO^- \rightarrow NO_3^- + 5\ H^+ + 4\ Cl^-$	$k = 2.31\times10^{2}$ L/mol/sec (25°C)	(Jafvert and Valentine, 1992)	(A14)
$CO(NH_2)_2 + Cl_2 \rightarrow CONH_2NHCl + H_2O$	$k = 3.10\times10^{7}$ L/mol/sec	U90, U_DL_710	(U1_Cl2)
$HOCl + CO(NH_2)_2 \rightarrow CONH_2NHCl + H_2O$	$k = 8.44\times10^{-2}$ L/mol/sec	U90, U_DL_710	(U1_HOCl)
$HOCl + CONH_2NHCl \rightarrow CO(NHCl)_2 + OH^-$	$k>10^{14}$ L/mol/sec	(Blatchley and Cheng, 2010)	(U2)
$HOCl + CO(NHCl)_2 \rightarrow NCl_2CONHCl + OH^-$	$k>10^{15}$ L/mol/sec	(Blatchley and Cheng, 2010)	(U3)
$HOCl + NCl_2CONHCl \rightarrow CO(NCl_2)_2 + OH^-$	$k>10^{15}$ L/mol/sec	(Blatchley and Cheng, 2010)	(U4)
$HOCl + CO(NCl_2)_2 \rightarrow CO_2 + NHCl_2 + NCl_3$	$k>10^{15}$ L/mol/sec	(Blatchley and Cheng, 2010)	(U5)
$C_4H_7N_3O + ClO^- \rightarrow C_4H_6N_3OCl + OH^-$	$k = 0.260$ L/mol/sec	C30, C90, C_B_10	(C1)
$C_4H_6N_3OCl + ClO^- + H_2O \rightarrow C_4H_8N_3O_2Cl + Cl^-$	$k>10^{15}$ L/mol/sec	C30, C90, C_B_10	(C2)
$C_4H_8N_3O_2Cl + H_2O \rightarrow CO(NH_2)_2 + CH_3NClCH_2COOH$	$k=65.7\ sec^{-1}$	C30, C90, C_B_10	(C3)
$CH_3NClCH_2COOH + ClO^- \rightarrow CH_3NCl_2 + CH3COOH$	$k>10^{15}$ L/mol/sec	C30, C90, C_B_10	(C4)
$CH3COOH + HOCl \rightarrow 0{,}007\ TCM$	$k = 0.01$ L/mol/sec	C30, C90	(C5)
$C_6H_9N_3O_2 + HOCl \rightarrow C_6H_8N_3O_2Cl + H_2O$	$k = 0.586$ L/mol/sec	H5, H10, H30S, H60, H90S	(H1)
$HOCl + C_6H_8N_3O_2Cl \rightarrow C_6H_7N_3O_2Cl_2 + H_2O$	$k=0.513$ L/mol/sec	H5, H10, H30S, H60, H90S	(H2)
$C_6H_7N_3O_2Cl_2 \rightarrow C_5H_7N_3Cl + CO_2 + Cl^-$	$k = 0.167\ sec^{-1}$	H5, H10, H30S, H60, H90S	(H3)
$C_6H_7N_3O_2Cl_2 \rightarrow C6H6N_3O_2Cl + H^+ + Cl^-$	$k = 0.325\ sec^{-1}$	H5, H10, H30S, H60, H90S	(H3bis)
$C_5H_7N_3Cl \rightarrow C_5H_5N_3 + H^+ + Cl^-$	$k = 7.04\times10^{-4}\ sec^{-1}$	H5, H10, H30S, H60, H90S	(H4)
$C_6H_6N_3O_2Cl \rightarrow C_5H_5N_3 + CO_2 + Cl^-$	$k = 1.00\times10^{-8}\ sec^{-1}$	H5, H10, H30S, H60, H90S	(H4bis)
$C_5H_5N_3 \rightarrow DCAN$	$k = 6.64\times10^{-4}\ sec^{-1}$	H5, H10, H30S, H60, H90S	(H5)
$C_6H_8N_3O_2Cl \rightarrow C_5H_7N_3 + CO_2 + Cl^-$	$k = 7.91\times10^{-8}\ sec^{-1}$	H30, H90	(H6)
$C_5H_7N_3 \rightarrow TCM + K$	$k = 1.10\times10^{-2}\ sec^{-1}$	H30, H90	(H7)
$HOCl + C_6H_5O_7 \rightarrow C_5H_4O_5 + CO_2 + H^+ + Cl^- + OH^-$	$k = 5.50\times10^{-3}$ L/mol/sec	CA10, CA30, CA65, CA90S, CA90, CA_B_20	(CA1)
$2\ HOCl + C_5H_4O_5 \rightarrow C_5H_4O_5Cl_2 + 2\ OH^-$	$k>10^{15}$ $L^2/mol^2/sec$	CA10, CA30, CA65, CA90S, CA90, CA_B_20	(CA2)
$C_5H_4O_5Cl_2 + OH^- \rightarrow HCO_3^- + C_4H_2O_3Cl_2$	$k>10^{15}$ L/mol/sec	CA10, CA30, CA65, CA90S, CA90, CA_B_20	(CA3)
$C_4H_2O_3Cl_2 + HOCl \rightarrow C_4H_2O_3Cl_3 + OH^-$	$k>10^{15}$ L/mol/sec	CA10, CA30, CA65, CA90S, CA90, CA_B_20	(CA4)

$C_4H_2O_3Cl_3$ + OH^- -> TCM + $C_3H_3O_3$	k>10^{15} L/mol/sec	CA10, CA30, CA65, CA90S, CA90, CA_B_20	(CA5)
HOCl + $C_5H_4N_4O_3$ -> $C_5H_4N_4O_4Cl$	k= 5.31 L/mol/sec	UA5, UA_L_20, UA_L_30	(UA1)
HOCl + $C_5H_4N_4O_4Cl$ -> $C_4H_5N_4O_3$ + CO_2	k>10^{15} L/mol/sec	UA5, UA_L_20, UA_L_30	(UA2)
$C_4H_5N_4O_3$ + 6 HOCl -> A + 0.05 CNCl + 0.035 NCl_3 + 0.063 TCM	k>10^{15} L/mol/sec	UA5, UA90, UA_L_30	(UA3)
HOCl + $C_9H_9NO_3$ -> $C_9H_9NO_4Cl$	k= 2.23 L/mol/sec	HA5, HA30	(HA1)
$C_9H_9NO_4Cl$ -> 0.018 TCM	k=4.08×10^{-6} sec^{-1}	HA5, HA30	(HA2)
DCAN + ClO^- -> ClDCAM	k=0.29 L/mol/sec	(Yu and Reckhow, 2017)	(DCAN1)
DCAN + OH^- -> DCAM	k=1.55 L/mol/sec	(Yu and Reckhow, 2017)	(DCAN2)
ClDCAM + HOCl -> DCAA + $NHCl_2$	k= 0.20 L/mol/sec	(Yu and Reckhow, 2017)	(DCAN3)
DCAM + ClO^- -> ClDCAM	k= 27.6 L/mol/sec	(Yu and Reckhow, 2017)	(DCAN4)
DCAM + OH^- -> DCAA	k=0.17 L/mol/sec	(Yu and Reckhow, 2017)	(DCAN5)

*Sources are given for rate constants taken from the literature. References of the experiments used for rates adjustment are precised for the rates determined in this study. If experimental data used for the adjustment come from another published paper, the experiment reference is indicated in bold. P = unidentified reaction products; I = unidentified intermediate.

2. Results and discussion

2.1. Chlorine consumption

Chlorine demand has been determined during a long-term experiment involving a contact time of 270 hr. Free chlorine rapidly decreased during the BFA chlorination experiment. The high initial chlorine doses were calibrated to ensure a residual chlorine concentration during long-term experiments. After 100 hr of reaction, 65 mg/L of free chlorine had been consumed. Then the free chlorine concentration decreased very slowly due to chlorine degradation. The BFA chlorine demand was estimated at 15 mg Cl_2/mg C. This value is close to the 18 mg Cl_2/mg C reported by Kanan and Karanfil,(2011) for the same BFA at 26°C and pH = 7. The BFA chlorine demand is higher than the chlorine demand of humic substances which is estimated at 1.1 – 2.3 mg Cl_2/mg C (Reckhow et al., 1990). Consequently, the filling water chlorine demand can be neglected compared to the chlorine consumption caused by the anthropogenic pollution in pools. The BFA components were individually chlorinated at chlorine doses of 30 mg/L of Cl_2 and 90 mg/L of Cl_2 with contact times of 170 hr and 270 hr respectively. Urea consumed 54 mg/L of Cl_2 after 270 hr of chlorination at 90 mg/L, which amounts to 78% of the total BFA chlorine demand (**Fig. 1a** and Appendix A S2). The ammonia molar chlorine demand, 1.7 mol/mol, is in good agreement with the value of 1.5 mol/mol proposed by the breakpoint model.

L-histidine chlorine demand was estimated at 10 mol/mol after 170 hr of reaction, which is slightly lower than the 12 mol/mol reported by Hureiki et al. (1994) and slightly higher than the 8 mol/mol measured by Li and Blatchley (2007) and Li et al. (2017). The 6 mol/mol reported here for creatinine chlorine demand are higher than the value of 2 mol/mol reported by Tachikawa et al. (2005) and Li and Blatchle (2007). It could be explained by different contact times (150 hr in this study). With a molar chlorine demand of 7 mol/mol, uric acid is one of the most chlorine consuming component but its contribution to the BFA total chlorine demand is limited due to its low concentration in the solution. Citric acid contribution is also low. Dickenson et al. (2008) reported 0.5 mol/mol after 24 hr contact time. In this study, the value was estimated at 4 mol/mol after 160 hr reaction. Although this value is comparable to the molar values of other components, the contribution of citric acid to the BFA chlorine consumption (1%) is low because of the low concentration of citric acid in the BFA solution. Little data is available concerning the chlorine demand of hippuric acid. After 150 hr reaction, hippuric acid had the lowest molar chlorine demand among the BFA components (1 mol/mol; 0.7% of the BFA chlorine demand).

Although urea has the highest chlorine demand in the BFA, note that its contribution to the chlorine consumption increases during the first 20 hr of reaction. Indeed, ammonia reacts more quickly than the other components including urea, which leads to a higher contribution (40%) to chlorine consumption at the beginning of the reaction.

L-histidine was found to consume very little chlorine during the first 3 hours of reaction at a chlorine to L-Histidine ratio of 10. Thus, its contribution to the overall BFA consumption at the beginning of the reaction may not be significant compared to urea's consumption. Lian et al. reported that uric acid reacts very quickly with chlorine. Its consumption rate is similar to the consumption rate of glycine. At a chlorine to uric acid molar ratio of 6.4, 85% of free chlorine were consumed after 60 min (Lian et al., 2014).

The model also includes a reaction representing chlorine degradation in the medium (Reaction (8), **Table 2**). The associated kinetic rate, included in the model, was calibrated on a long term experiment at the initial chlorine dose of 90 mg/L and is in agreement with the rate proposed by Lister (1956) for sodium hypochlorite decomposition ($k = 3.8\times10^{-7}$ sec^{-1}).

a

BFA component	Chlorine demand (mg/L of Cl_2)	Chlorine demand (mol /mol)	Concentration (mmol/L)	Contribution to the BFA chlorine demand (%)
Ammonium chloride	3.5	1.7	2.88×10^{-2}	5.1
Urea	54	4	1.90×10^{-1}	78
Creatinine	5.2	6	1.23×10^{-2}	7.5
L-Histidine	4.3	10	6.01×10^{-3}	6.2
Citric acid	0.7	4	2.57×10^{-3}	1.0
Uric acid	1.1	7	2.24×10^{-3}	1.6
Hippuric acid	0.50	1	7.35×10^{-3}	0.70

b

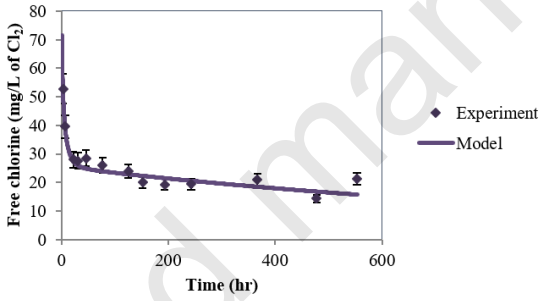

Fig. 1 Chlorine demand of the BFA solution and of its components. (a) BFA demand vs individual components demand measured after 270 hr chlorination with an initial chlorine dose of 90 mg/L of Cl_2, pH = 7.5, T = 27°C, (b) Modeling of the BFA chlorine consumption and experimental results (n=3) for an initial chlorine dose of 90 mg/L of Cl_2, pH = 7.5, T = 27°C

Urea chlorination has been widely documented. The chlorination mechanism has been proposed by Samples (1959), then modified by Blatchley and Cheng (2010), who suggested that the first step, which is rate-limiting, involves molecular chlorine rather than hypochlorous acid. Blatchley and Cheng (2010) also measured a rate constant for this first step by monitoring the N-chlorourea concentration spectrophotometrically at λ = 245 nm and pH = 2.0. However, the mechanism proposed with this rate did not fit with the experimental data of this study (**Fig. 2**). The residual chlorine concentration following 600 hr of reaction and estimated with this model reached 0.045 mg/L of Cl_2, whereas long term experiments exhibited a residual concentration of 15 mg/L of Cl_2 for the same duration. Hence, urea chlorination by hypochlorous acid was

taken into account and a rate constant was fitted. As a result of this change, the reaction rate of Cl_2 with urea was also reassessed. The reaction rate of urea chlorination by HOCl was estimated at 8.44×10^{-2} L/mol/sec, whereas the reaction rate with Cl_2 was calculated at 3.10×10^{7} L/mol/sec. These values confirm that Cl_2 reacts more quickly with urea than HOCl.

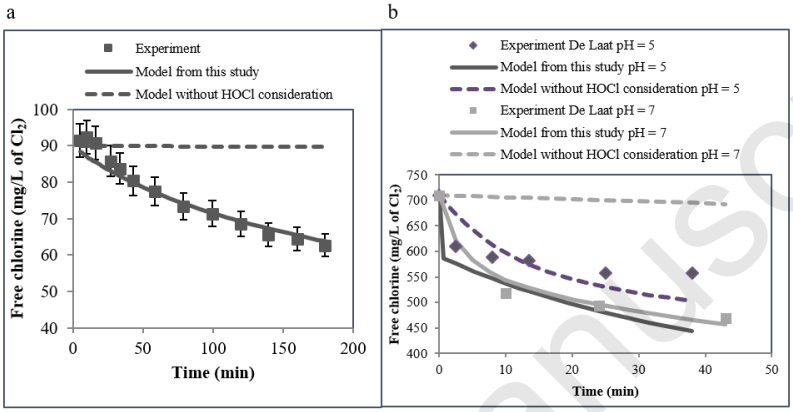

Fig. 2 Urea chlorination and comparison of models with and without HOCl consideration at different initial chlorine concentrations and pH. (a) Experimental data (n = 3) at initial Cl_2 concentration 90 mg/L, initial urea concentration 0.19 mmol/L, temperature 27°C, pH 7.5. (b) initial Cl_2 concentration 710 mg/L, initial urea concentration 1 mmol/L temperature 25°C, pH 7 or 5.4 (data from De Laat et al., 2011)

Urea consumed 3.8 mol/mol at pH = 7.5, which is consistent with the literature data (De Laat et al., 1982). However De Laat (2011) observed that this value is pH-dependent: at pH = 4.5 urea chlorine demand reaches 2.5 mol/mol urea. The model presented here could not fit for pH-value out of the range 6.5 - 8.

Chlorine demand for other components and examples of chlorine consumption fits are reported in Appendix A S2.

2.2. Chloroform formation

2.2.1. Chloroform formation from the BFA components

All BFA components were individually chlorinated at 30 and 90 mg/L of Cl_2 during 150 hr and 270 hr respectively. For some components, specific chlorination experiments at lower initial chlorine doses were performed (Appendix A S3).

Very different TCM molar yields were obtained from the chlorination experiments of BFA components. However, urea, creatinine, L-histidine and uric acid have similar contributions (3% – 5%) due to their different concentrations in the BFA mix (**Table 3**). TCM amounts formed by citric acid were significantly higher than the concentrations produced by the other components. For example, urea and creatinine formed 10 µg/L of TCM (0.084 µmol/L) after 150 hr chlorination at 90 mg/L, which involves formation potentials of 4.2×10^{-4} mol/mol and 7.2×10^{-3} mol/mol for urea and creatinine respectively. After the same contact time citric acid chlorination produced 250 µg/L of TCM (2.1 µmol/L) (Appendix A S3). One mole of citric acid produced 120 times more chloroform than one mole of creatinine and 2000 times more chloroform than one mole of urea. The ability of citric acid to form higher quantities of TCM than other BFA components has been reported in numerous studies (Blatchley et al., 2003; Dickenson et al., 2008), with yields varying between 50% and 80% (Blatchley et al., 2003; Larson and Rockwell, 1979). Regarding the TCM formation potential determined in this study, it appears that citric acid is the main precursor for TCM in the BFA. Citric acid is responsible for 80% of the TCM formed during BFA chlorination. In fact, the total TCM quantity yielded by the BFA components excluding citric acid was in the same order of magnitude as the measurement uncertainty. Only hippuric acid yielded significant TCM quantities.

Table 3 Chloroform formation from the BFA components.

BFA component	Concentration (mmol/L)	Yield of TCM formation (mmol/mol)	Contribution to the TCM production from BFA chlorination (%)
Ammonium chloride	2.88×10^{-2}	0	0
Urea	1.90×10^{-1}	0.40	2.7
Creatinine	1.23×10^{-2}	7.20	3.0
L-Histidine	6.01×10^{-3}	24.0	5.1
Citric acid	2.57×10^{-3}	881	77
Uric acid	2.24×10^{-3}	63.4	4.9
Hippuric acid	7.35×10^{-3}	28.5	7.2

Initial Cl_2 concentration 90 mg/L, pH 7.5, temperature 27°C.

2.2.2. Citric acid chlorination modeling

Citric acid was chlorinated at 90 mg/L during 270 hr in UPW at 27°C. 2.5 µmol/L TCM were formed during this experiment, which implies a TCM formation potential of 0.9 ± 0.2 mol/mol for citric acid.

A chlorination mechanism has been proposed by Larson and Rockwell (1979), in which the first step leads to the formation of 3-ketoglutaric acid by citric acid decarboxylation. 3-Ketoglutaric acid yields large amounts of TCM by undergoing the haloform reaction (Deborde and von Gunten, 2008; Dickenson et al., 2008; Fuson and Bull, 1934). The resulting chlorination mechanism proposed in this study is shown in Appendix A S4. Larson and Rockwell (1979) proposed a rate-limiting decarboxylation step based on the finding that the optimum pH corresponds to the simultaneous presence of the citrate trianion and of the hypochlorous acid. Acid-base equilibria of citric acid were included in the model *via* Reactions (5), (6) and (7) (**Table 2**). Considering the much higher yield observed by Larson and Rockwell (1979) at pH = 7, it was supposed that the citrate trianion was the only form reacting with hypochlorous acid. For the same reason it was supposed that hypochlorous acid was the only chlorine specie involved in the reaction. No kinetic rate was proposed in previous studies for the decarboxylation step. In this study the first kinetic rate was fitted with data obtained from experiments performed at different initial chlorine doses (**Table 2** and Appendix A S3). The experimental data published by Blatchley et al. (2003), were also used to fit the rate with experiments performed at a different citric acid concentration. The reaction rate was established at 5.50×10^{-3} L/mol/sec.

Fig. 3 presents the main results of kinetic modeling. It can be observed that the model fits with experimental points for long-term experiments (350 hr) as well as for short term experiments (10 hr). However, the values predicted by the model are 15% to 20% lower than the experimental data from Blatchley et al. (2003).

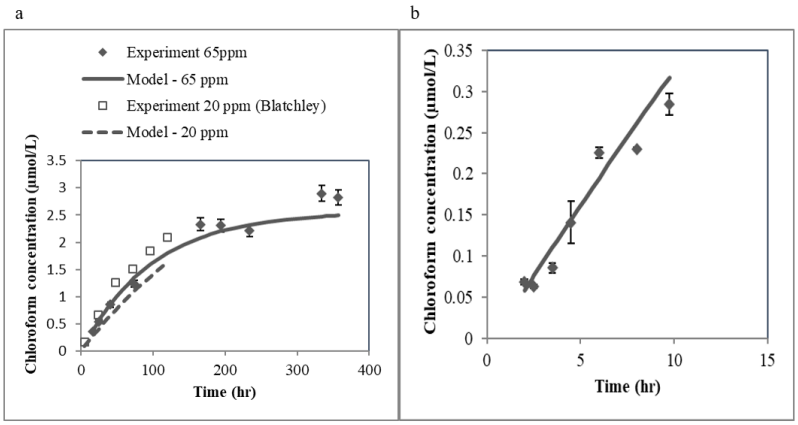

Fig. 3 Chloroform formation from citric acid chlorination. (a) Citric acid (2.6×10^{-6} mol/L) chlorination at 65 mg/L Cl_2, temperature 27°C, pH 7.5 (n = 3) and model (full line). Citric acid (5.2×10^{-6} mol/L) chlorination at 20 mg/L Cl_2, temperature 25°C, pH 7.0, experimental data from Blatchley et al. (2003 and model (dashed line). (b) Focus on the beginning of the chlorination reaction of citric acid (2.6×10^{-6} mol/L) at 90 mg/L Cl_2, temperature 27°C, pH 7.5 (n = 3).

A very long-term experiment was performed on BFA and citric acid at 90 mg/L to evaluate chloroform formation for contact times longer than 1500 hr (**Fig. 4**). The mean concentration measured for chloroform was 1.3 µmol/L. Although the experimental values are dispersed, a clear decreasing trend can be observed for long contact times, which suggests a loss during the experiments. Moreover, gas bubbles and thus headspace formation were observed in the bottles during the experiments. This phenomenon could be explained by the gas formed as reactions by-products (N_2, CO_2), and it could lead to the loss of TCM. UPW could also degas and participate in the bubble formation. To take this loss into account in the model, a loss rate was fitted with the results of a dedicated experiment and it was validated with long term experiments performed on BFA and citric acid.

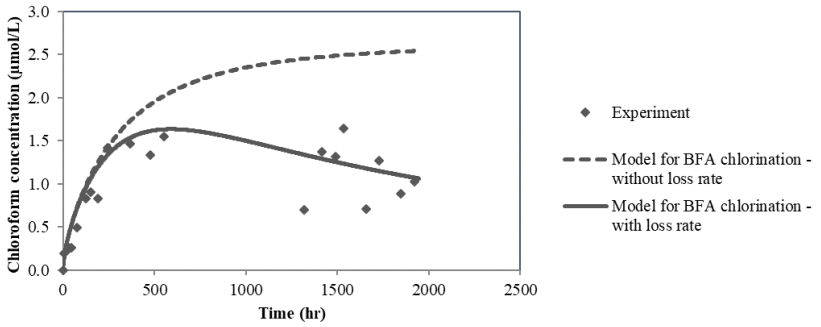

Fig. 4 Modeling chloroform formation kinetics from BFA chlorination and loss. Initial Cl_2 concentration 90 mg/L, temperature 27°C.

The other BFA components contributions were also modeled, based on the experiments presented in Appendix A S3. The results presented in **Fig. 5** show that the predicted overall chloroform concentration is slightly higher than the measured concentration. The minor contributions are, as said, in the same range as the experimental uncertainty. However, it is noticeable that the TCM formation rates of the BFA components are different. Urea, creatinine, L-histidine and uric acid contributions were mainly formed within the first 150 hr of reaction. On the contrary, the contribution of hippuric acid was not visible during the first 50 hr of reaction.

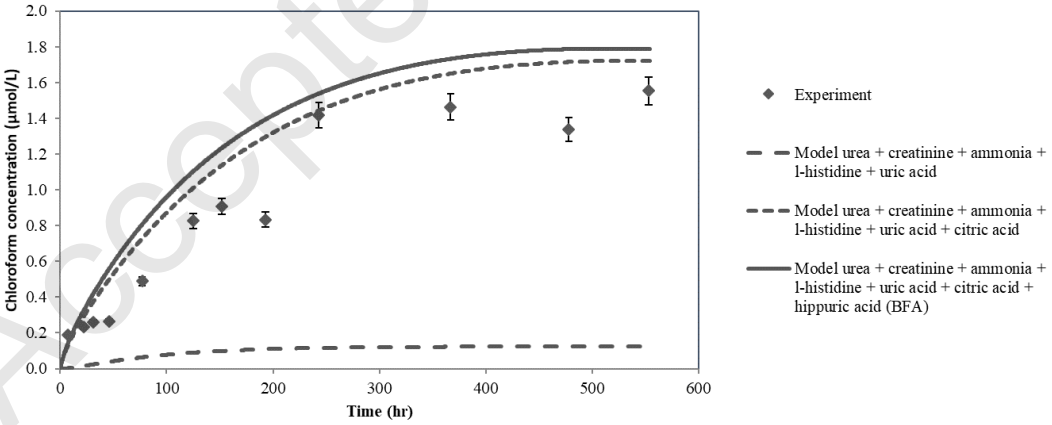

Fig. 5 Modeling the chloroform formation from chlorination of BFA components. Initial Cl_2 concentration 90 mg/L, temperature 27°C, n = 3.

2.3. Dichloroacetonitrile formation kinetics

2.3.1. DCAN formation from the BFA chlorination

The BFA was chlorinated at different initial chlorine doses and the DCAN formation was monitored during the first 24 hr of reaction. DCAN is not stable in the aqueous media. Indeed, it is easily degraded by hydrolysis and by reaction with hypochlorite to form dichloroacetamide and N-chloro-2,2-dichloroacetamide respectively (Glezer et al., 1999; Yu and Reckhow, 2015). The DCAN produced by the BFA chlorination reached a maximum concentration of 0.9 µmol/L before starting to decrease (Appendix A S5, Fig. S30)

Few articles address the relative DCAN formation potentials of BFA components. In this study, all BFA components were individually chlorinated at 90 mg/L and the DCAN was monitored during the first 10 hr of reaction. DCAN was detected only during L-histidine chlorination. However, DCAN formation was different whether the L-histidine was isolated or in the BFA solution. The BFA chlorination yielded immediately high amounts of DCAN from the beginning of the chlorination. On the contrary, during isolated L-histidine chlorination experiments, the DCAN concentration started to increase quickly after 2 hr of reaction (Appendix A S5).

2.3.2. DCAN formation from L-histidine chlorination

L-histidine produced large amounts of DCAN by reaction with chlorine. The maximum concentration measured during L-histidine chlorination at 90 mg/L was 1 µmol/L, or 166.6 mmol/mol, which is very close to the maximum DCAN concentration observed during BFA chlorination (0.9 µmol/L). Note that for high initial chlorine doses (above 60 mg/L) the DCAN concentration increased very slowly during the first 2 hr and then sharply increased to reach a peak before decreasing due to DCAN degradation (**Fig. 6**).

L-histidine reactivity with chlorine has been studied previously within the scope of amino-acids chlorination. Amino-acids generally form high quantities of DCAN because of the amine group which facilitates the decarboxylation step leading to the formation of the nitrile group (Shah and Mitch, 2012; Trehy et al., 1986). Note that combined amino-acids derived from the condensation of two or more amino-acids, were proven to produce lower amounts of DCAN

than free amino-acids, while having a lower molar chlorine demand (Hureiki et al., 1994; Li et al., 2017). In the case of combined amino-acids, the nitrogen is indeed engaged into an amide bound, making it less available for the decarboxylation reaction. In the case of L-histidine, Li and Blatchley (2007) also pointed out the possible chlorination of the secondary amine located on the ring.

No kinetic rate has been proposed before for the formation of DCAN from L-histidine chlorination. However, Yu and Reckhow (2017, 2015) reported complete degradation mechanism and degradation kinetics of DCAN, which was in good agreement with experimental results of this study. Hence, their rate constants were directly included in the model to take this degradation into account.

Li et al. (2017) proposed a chlorination mechanism of L-histidine explaining the formation of both DCAN and TCM. This mechanism was considered for kinetic rate fitting (Appendix A S4). The kinetic rates of reactions (H1) to (H7) were obtained by fitting the mechanism with chlorination experiments of L-histidine at 5, 10, 30, 60 and 90 mg/L of Cl_2 (**Table 2** and Appendix A S5). Reactions (H1) to (H5) were fitted on experiments H5, H10, H60, H30S, H90S. These experiments were specifically designed for the monitoring of DCAN, which degradation implies short contact times. Reactions (H6) and (H7) were fitted on experiments H5, H10, H30 and H90, whose contact times were longer. All the fitted models included the degradation rates determined by Yu and Reckhow (2017, 2015).

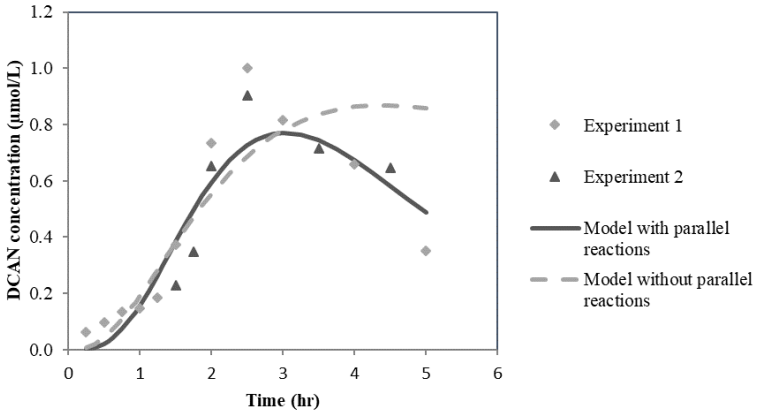

Fig. 6 Modelling results for the dichloroacetonitrile formation from L-histidine chlorination, Initial Cl_2 concentration 90 mg/L, pH 7.5, temperature 27°C

The model fits satisfactorily with the experiments, considering the sudden slope changes observed. The presence of two parallel ways of reaction leading to the formation of the nitrile group in the mechanism is in agreement with the kinetic modeling since the presence of these parallel ways improves significantly the fit for the experiments with high initial chlorine doses (60 and 90 mg/L) compared to a linear mechanism (**Fig. 6**).

To further investigate the DCAN formation mechanism and the reactivity of L-histidine in the BFA, chlorination experiments of BFA components mixtures at 90 mg/L were performed. The BFA components concentrations were the same as in the BFA. **Fig. 7** shows the evolution of DCAN concentration for different mixtures.

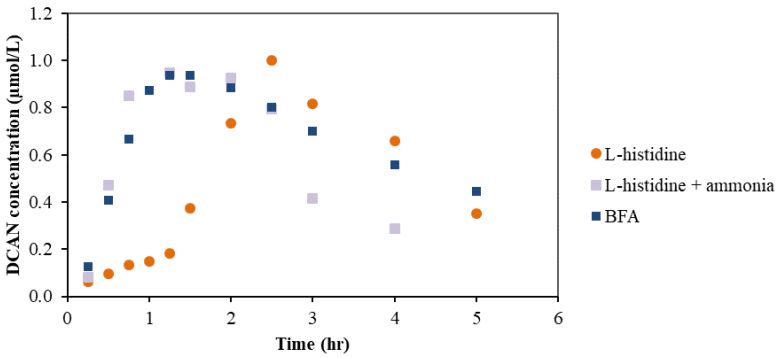

Fig. 7 Dichloroacetonitrile formation from L-histidine, L-histidine + ammonia and BFA chlorination. Initial Cl_2 concentration 90 mg/L, temperature 27°C, pH 7.5.

Ammonia or one of its chlorination by-products may accelerate the DCAN formation during the L-histidine chlorination. The mechanism proposed previously (Li et al., 2017; Li and Blatchley, 2007; Liu et al., 2017) does not allow to explain the role of ammonia. This point should be further investigated to build a kinetic model explaining these differences of reactivity.

3. Conclusion

In this work, an original kinetic model has been established for the prediction of chlorine consumption, chloroform formation and dichloroacetonitrile formation. The BFA chlorine demand was estimated at 15 mg Cl_2/mg TOC, which is considerably higher than the chlorine demand of natural organic matter. Urea was found to be responsible for 78% of the BFA chlorine demand. The first step of urea chlorination is confirmed to be rate-limiting, and the contributions of both HOCl (k= 8.44×10^{-2} L/mol/sec) and Cl_2 (k= 3.10×10^{7} L/mol/sec) were considered in order to obtain a good fitting. It is noteworthy that the contribution of ammonia at the beginning of the reaction is significant because of its high reactivity. Chloroform is slowly formed (k=5.50×10^{-3} L/mol/sec), mainly by citric acid chlorination, which contributes to almost 80% of the chloroform formation potential of the BFA. The model of chloroform formation was calibrated on several experiments including a wide range of contact times as well as data of the literature. Dichloroacetonitrile was formed by the chlorination of L-histidine which is the only precursor for this by-product. The kinetic model for L-histidine chlorination was fitted with the latest published chlorination mechanism and different reactivities were observed for L-histidine depending on its environment. The presence of ammonia seemed to catalyze the

formation of dichloroacetonitrile, but further information about L-histidine chlorination mechanism is required to fully explain the chlorination kinetics of this molecule.

Acknowledgments

The authors would like to acknowledge the Conseil Régional de Bretagne for financial support. They also would like to express their sincere thanks to colleagues who improved the quality of this document.

Appendix A. Supplementary data

Supplementary data associated with this article can be found in the online version at xxxxxx.

References

APHA, 2005. Standard Methods for the examination of water and wastewater, 21rst ed. American Public Health Association, Washington, DC.

Arnold, W.A., Bolotin, J., Gunten, U. von, Hofstetter, T.B., 2008. Evaluation of Functional Groups Responsible for Chloroform Formation during Water Chlorination Using Compound Specific Isotope Analysis. Environ. Sci. Technol. 42, 7778–7785. https://doi.org/10.1021/es800399a

Bates, R.G., Pinching, G.D., 1949. Resolution of the dissociation constants of citric acid at 0 to 50°, and determination of certain related thermodynamic functions. J. Am. Chem. Soc. 71, 1274–1283.

Beech, J.A., 1980. Estimated worst case trihalomethane body burden of a child using a swimming pool. Med. Hypotheses 6, 303–307.

Bessonneau, V., Derbez, M., Clément, M., Thomas, O., 2011. Determinants of chlorination by-products in indoor swimming pools. Int. J. Hyg. Environ. Health 215, 76–85. https://doi.org/10.1016/j.ijheh.2011.07.009

Blatchley, E.R., Cheng, M., 2010. Reaction Mechanism for Chlorination of Urea. Environ. Sci. Technol. 44, 8529–8534. https://doi.org/10.1021/es102423u

Blatchley, E.R., Margetas, D., Duggirala, R., 2003. Copper catalysis in chloroform formation during water chlorination. Water Res. 37, 4385–4394. https://doi.org/10.1016/S0043-1354(03)00404-4

Connick, R.E., Chia, Y.T., 1959. The hydrolysis of chhlorine and its variation with temperature. J. Am. Chem. Soc. 81, 1280–1284.

De Laat, J., Feng, W., Freyfer, D.A., Dossier-Berne, F., 2011. Concentration levels of urea in swimming pool water and reactivity of chlorine with urea. Water Res. 45, 1139–1146. https://doi.org/10.1016/j.watres.2010.11.005

De Laat, J., Merlet, N., Dore, M., 1982. Chlorination of organic compounds : chlorine demand and reactivity in relationship to the trihalomethane formation. Water Res. 16, 1437–1450.

Deborde, M., von Gunten, U., 2008. Reactions of chlorine with inorganic and organic compounds during water treatment—Kinetics and mechanisms: A critical review. Water Res. 42, 13–51. https://doi.org/10.1016/j.watres.2007.07.025

Dickenson, E.R.V., Summers, R.S., Croué, J.-P., Gallard, H., 2008. Haloacetic acid and Trihalomethane Formation from the Chlorination and Bromination of Aliphatic β-

Dicarbonyl Acid Model Compounds. Environ. Sci. Technol. 42, 3226–3233. https://doi.org/10.1021/es0711866
Erdinger, L., Kühn, K.P., Kirsch, F., Feldhues, R., Fröbel, T., Nohynek, B., Gabrio, T., 2004. Pathways of trihalomethane uptake in swimming pools. Int. J. Hyg. Environ. Health 207, 571–575.
Florentin, A., Hautemanière, A., Hartemann, P., 2011. Health effects of disinfection by-products in chlorinated swimming pools. Int. J. Hyg. Environ. Health 214, 461–469. https://doi.org/10.1016/j.ijheh.2011.07.012
Fuson, R.C., Bull, B.A., 1934. The Haloform Reaction. Chem. Rev. 15, 275–304.
Gérardin, F., Cloteaux, A., Midoux, N., 2015. Modeling of variations in nitrogen trichloride concentration over time in swimming pool water. Process Saf. Environ. Prot. 94, 452–462. https://doi.org/10.1016/j.psep.2014.10.004
Glezer, V., Batsheva, H., Tal, N., Iosefzon, B., Lev, O., 1999. Hydrolysis of haloacetonitriles : linear free enegy relationship, kinetics and products. Water Res. 33, 1938–1948.
Hureiki, L., Croue, J.-P., Legube, B., 1994. Chlorination studies of free and combined amino acids. Water Res. 28, 2521–2531.
Jafvert, C.T., Valentine, R.L., 1992. Reaction scheme for the chlorination of ammoniacal water. Environ. Sci. Technol. 26, 577–585.
Judd, S.J., Black, S.H., 2000. Disinfection by-product formation in swimming pool waters a simple mass balance. Water Res. 34, 1611–1619.
Judd, S.J., Bullock, G., 2003. The fate of chlorine and organic materials in swimming pools. Chemosphere 51, 869–879. https://doi.org/10.1016/S0045-6535(03)00156-5
Kanan, A., Karanfil, T., 2011. Formation of disinfection by-products in indoor swimming pool water: The contribution from filling water natural organic matter and swimmer body fluids. Water Res. 45, 926–932. https://doi.org/10.1016/j.watres.2010.09.031
Keuten, M.G.A., Schets, F.M., Schijven, J.F., Verberk, J.Q.J.C., van Dijk, J.C., 2012. Definition and quantification of initial anthropogenic pollutant release in swimming pools. Water Res. 46, 3682–3692. https://doi.org/10.1016/j.watres.2012.04.012
Kim, H., Han, K., 2011. Swimmers contribute to additional formation of N-nitrosamines in chlorinated pool water. Toxicol. Environ. Health Sci. 3, 168–174. https://doi.org/10.1007/s13530-011-0094-1
Kim, H., Shim, J., Lee, S., 2002. Formation of disinfection by-products in chlorinated swimming pool water. Chemosphere 46, 123–130.
Larson, R.A., Rockwell, A.L., 1979. Chloroform and chlorophenol production by decarboxylation of natural acids during aqueous chlorination. Environ. Sci. Technol. 13, 325–329.
Lévesque, B., Ayotte, P., Leblanc, A., Dewailly, E., Prud'Homme, D., Lavoie, R., Allaire, S., Levallois, P., 1994. Evaluation of dermal and respiratory chloroform exposure in humans. Environ. Health Perspect. 102, 1082–1087.
Li, C., Gao, N., Chu, W., Bond, T., Wei, X., 2017. Comparison of THMs and HANs formation potential from the chlorination of free and combined histidine and glycine. Chem. Eng. J. 307, 487–495. https://doi.org/10.1016/j.cej.2016.08.110
Li, J., Blatchley, E.R., 2007. Volatile disinfection byproduct formation resulting from chlorination of organic-nitrogen precursors in swimming pools. Environ. Sci. Technol. 41, 6732–6739.
Lian, L., E, Y., Li, J., Blatchley, E.R., 2014. Volatile Disinfection Byproducts Resulting from Chlorination of Uric Acid: Implications for Swimming Pools. Environ. Sci. Technol. 48, 3210–3217. https://doi.org/10.1021/es405402r
Lister, M.W., 1956. Decomposition of sodium hypochlorite : the uncatalyzed reaction. Can. J. Chem. 34, 465–478.
Liu, Z., Chen, W., Yu, H., Tao, H., Xu, H., Yu, J., Gu, Y., Wan, Z., 2017. Effects of pre-oxidation and adsorption on haloacetonitrile and trichloronitromethane formation during subsequent chlorination. Environ. Sci. Pollut. Res. 24, 21836–21845. https://doi.org/10.1007/s11356-017-9843-2

Manasfi, T., Coulomb, B., Boudenne, J.-L., 2017a. Occurrence, origin, and toxicity of disinfection byproducts in chlorinated swimming pools: An overview. Int. J. Hyg. Environ. Health 220, 591–603. https://doi.org/10.1016/j.ijheh.2017.01.005

Manasfi, T., Temime-Roussel, B., Coulomb, B., Vassalo, L., Boudenne, J.-L., 2017b. Occurrence of brominated disinfection byproducts in the air and water of chlorinated seawater swimming pools. Int. J. Hyg. Environ. Health 220, 583–590. https://doi.org/10.1016/j.ijheh.2017.01.008

Morris, J.C., 1966. The acid ionization constant of HOCl from 5 to 35°C. J. Phys. Chem. 70, 3798–3805.

Peng, D., Saravia, F., Abbt-Braun, G., Horn, H., 2016. Occurrence and simulation of trihalomethanes in swimming pool water: A simple prediction method based on DOC and mass balance. Water Res. 88, 634–642. https://doi.org/10.1016/j.watres.2015.10.061

Putnam, D.F., 1971. Composition and concentrative properties of human urine. Natl. Aeronaut. Space Adm.

Qiang, Z., Adams, C.D., 2004. Determination of Monochloramine Formation Rate Constants with Stopped-Flow Spectrophotometry. Environ. Sci. Technol. 38, 1435–1444. https://doi.org/10.1021/es0347484

Reckhow, D.A., Singer, P.C., Malcolm, R.L., 1990. Chlorination of humic materials : byproducts formation and chemical interpretations. Environ. Sci. Technol. 24, 1655–1664.

Samples, W.R., 1959. A study on the chlorination of urea. Harvard University, Cambridge, MA.

Schmalz, C., Frimmel, F.H., Zwiener, C., 2011. Trichloramine in swimming pools – Formation and mass transfer. Water Res. 45, 2681–2690. https://doi.org/10.1016/j.watres.2011.02.024

Shah, A.D., Mitch, W.A., 2012. Halonitroalkanes, Halonitriles, Haloamides, and N-Nitrosamines: A Critical Review of Nitrogenous Disinfection Byproduct Formation Pathways. Environ. Sci. Technol. 46, 119–131. https://doi.org/10.1021/es203312s

Tachikawa, M., Aburada, T., Tezuka, M., Sawamura, R., 2005. Occurrence and production of chloramines in the chlorination of creatinine in aqueous solution. Water Res. 39, 371–379. https://doi.org/10.1016/j.watres.2004.09.029

Teo, T.L.L., Coleman, H.M., Khan, S.J., 2015. Chemical contaminants in swimming pools: Occurrence, implications and control. Environ. Int. 76, 16–31. https://doi.org/10.1016/j.envint.2014.11.012

Trehy, M.L., Yost, R.A., Miles, C.J., 1986. Chlorination Byproducts of Amino Acids in Natural Waters. Environ. Sci. Technol. 20, 1117–1122.

Weil, I., Morris, J.C., n.d. Equilibrium Studies on N-Chloro Compounds. II. The Base Strength of N-Chloro Dialkylamines and of Monochloramine. Artic. Présenté Au Natl. Res. Counc. I6 1949.

WHO, 2006. Guidelines for safe recreational water, vol. 2.

Yu, Y., Reckhow, D.A., 2017. Formation and Occurrence of *N-Chloro* -2,2-dichloroacetamide, a Previously Overlooked Nitrogenous Disinfection Byproduct in Chlorinated Drinking Waters. Environ. Sci. Technol. 51, 1488–1497. https://doi.org/10.1021/acs.est.6b04218

Yu, Y., Reckhow, D.A., 2015. Kinetic Analysis of Haloacetonitrile Stability in Drinking Waters. Environ. Sci. Technol. 49, 11028–11036. https://doi.org/10.1021/acs.est.5b02772

Zwiener, C., Richardson, S.D., De Marini, D.M., Grummt, T., Glauner, T., Frimmel, F.H., 2007. Drowning in Disinfection Byproducts? Assessing Swimming Pool Water. Environ. Sci. Technol. 41, 363–372. https://doi.org/10.1021/es062367v